MQP-BIO-DSA-3302

The Importance of Actin Interacting Proteins: dbn-1, erm-1, plst-1, and F38E9.5 for Pore Forming Toxin Defense in C. elegans

A Major Qualifying Project Report

Submitted to the Faculty of the

WORCESTER POLYTECHNIC INSTITUTE

in partial fulfillment of the requirements for the

Degree of Bachelor of Science

in

Biology and Biotechnology

by

Tammy Zamaitis

April 28, 2016

APPROVED:

Raffi Aroian, PhD
Department of Molecular Medicine
UMass Medical School
MAJOR ADVISOR

David Adams, PhD
Biology and Biotechnology
WPI Project Advisor

ABSTRACT

The Aroian lab previously identified a list of differentially regulated proteins when *Caenorhabditis elegans* was exposed to Cry5B. The actin-interacting proteins showed the most notable changes. Using genetic interacting assays with known pathways, hypersensitivity assays, pore repair assays, and endocytosis assays, we investigated the potential role of four actin-binding genes: dbn-1, erm1, plst-1, and F38E9.5. Knockdown of dbn-1, erm1, and plst-1 showed increased susceptibility to toxin Cry5B exposure than empty vector, suggesting these genes play a functional role in toxin defense.

TABLE OF CONTENTS

ACKNOWLEDGEMENTS

I would like to thank Dr. Raffi Aroian, a Principal Investigator in the Department of Molecular Medicine at the UMass Medical School, for the creation of this project and for providing his laboratory space and supplies for this project. I would also like to thank Dr. Anand Sitaram from UMass Medical School for not only teaching me the laboratory techniques required for this project, but also consistently providing me with advice and guidance throughout this research project. Finally, I would like to thank my WPI Project Advisor, Dr. Dave Adams for his continual patience, guidance, and support throughout this entire project as well as for helping edit and revise the report.

BACKGROUND

Bacteria play an essential role in the global ecosystem, occupying important niches in agriculture, environment, ecology, and medicine. Currently, about 4,500 species of bacteria have been characterized (Torsvik *et al.*, 2002). Although the vast majority of bacteria are harmless and even helpful, many strains cause disease. Pathogenic bacteria contribute to about 54.3% of emerging worldwide infectious diseases (Jones *et al*., 2008). Pore-forming toxins (PFTs) are a central theme in bacterial pathogenesis, as many bacterial pathogens produce PFTs as their main mode of infection (Geny and Popoff, 2006).

Pore-Forming Toxins

Pore-forming toxins are the most common and diverse class of bacterial protein exotoxins (Menestrina *et al*., 2011). These proteins have a broad taxonomic distribution, ranging from bacteria to mammals (Menestrina *et al*., 2011). Some well-known examples of pore-forming pathogenic bacterial strains include *Vibrio cholerae, Streptococcus pneumonia,* and *Staphylococcus aureu*s (Ladant *et al*., 2005). Bacterial PFTs are secreted toxins that damage the target's membrane (Geny and Popoff, 2006). Once secreted by a bacterial cell, PFTs function by binding to host receptors and converting from a water-soluble form to a transmembrane form that forms an oligomeric pore, and is inserted into the membrane (**Figure-1**) (Yamashita *et al*., 2014). These pores cause subsequent destruction of the osmotic equilibrium which eventually leads to leakage, cell lysis, and eventually organismal death (Geny and Popoff, 2006).

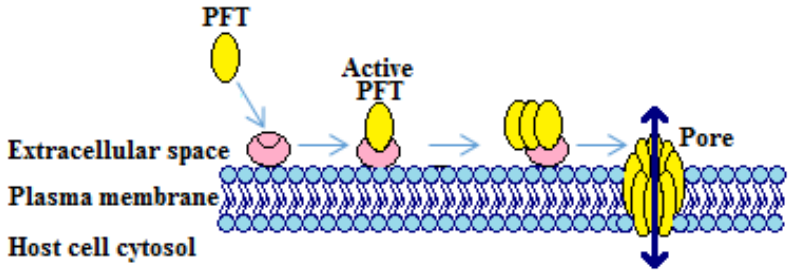

Figure 1. Generalized Mechanism of Pore-forming Toxins. The diagram shows a pore-forming toxin (yellow) binding to a receptor in the target cell membrane (pink), altering the conformation from a water-soluble form to a transmembrane form that creates a pore through which the cytoplasm leaks.

Classes of Pore-Forming Toxins

PFT's are classified into two main categories depending on the secondary structure of the toxin domain membrane that perforates the plasma membrane (Dal Peraro and Goot, 2016). The first category of PFTs is the *α*-PFTs, which form pores in the target's membrane by using an alpha helical layer (Jones *et al*., 2008). The second category of PFTs is the *β*-PFTs, which use β-sheets to form the pore in the target's plasma membrane (Gonzalez *et al*., 2008).

α-PFTs are secreted by many major pathogens including *Mycobacterium tuberculosis* and the cry toxins produced by *Bacillus thuringiensis* (Heuck and Johnson, 2005). The major, distinguishing structural pore feature of the α-PFTs (**Figure-2**) is comprised of 10 layered alpha helices that surround a hairpin loop (Gonzalez *et al*., 2008).

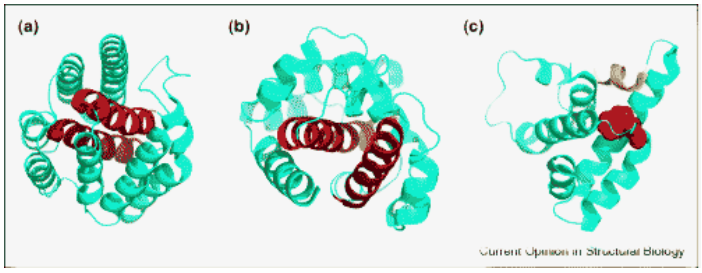

Figure-2: Example Structures of Three Types of α-Pore-Forming Domains. Shown are three α-PFTs: Colicin B (A), diphtheria toxin (B), and exotoxin A (C). The 10 layered alpha helices are represented in green, while the hairpin loop that is surrounded by the layered alpha helices is represented in red. Adapted from: Tilley and Saibil, 2006.

The exact mechanism of pore formation for this class of PFTs is still unclear; but it is thought that pore formation by α-PFTs requires three steps: binding, unfolding of the protein, and insertion of the hairpin loop (Tilley and Saibil, 2006). An inactive, soluble α-PFT first binds to a receptor on the target's plasma membrane. Low pH triggers the partial unfolding of the protein which exposes the hydrophobic hairpin structure (Parker and Feil, 2005). The hydrophobic hairpin structure is inserted into the lipid bilayer of the target membrane, and the remaining alpha pore-forming helices are inserted into the membrane (Parker and Feil, 2005).

The second category of PFTs is the β-pore-forming toxins; the majority of all known pore-forming toxins belong to this category (Iacovache, *et al*., 2006). The β-PFTs form the most well studied group of pore-forming toxins. Some well-known pathogenic bacterial strains that utilize β-PFTs as their mechanism of infection are *Aeromonas hydrophila* and *Staphylococcus aureus* (Iacovache, *et al*., 2006). The β-PFT family is named due to the *β*-barrel pore that forms in the target's plasma membrane (Jones *et al*., 2008). The *β*-PFTs function similarly to the α-PFTs. The *β*-PFTs are secreted by bacteria as a soluble protein and bind to receptors on the target's plasma membrane (Tilley and Saibil, 2006). Once bound to the receptors, the *β*-PFTs

oligomerize to refold the protein (Gonzalez *et al*., 2008). The re-folded proteins form the transmembrane *β*-barrel which crosses the lipid bilayer to form the active pore (Gonzalez *et al*., 2008). To form pore, the hemolysin subunit of the protein inverts to fold into the β-hairpin loops which forms the transmembrane *β*-barrel. The *β*-barrel is inserted into the target's membrane to form the pore (Tilley *et al*., 2006). Three example *β*-PFTs are shown in **Figure-3**. The *β*-barrel allows for insertion as it contains a hydrophobic outer surface and a hydrophilic core (Gonzalez *et al*., 2008). Interestingly, the size of the pore varies greatly between β-PFTs, and can range from about 2 nm to as large as 50 nm (Gonzalez, *et al*., 2008).

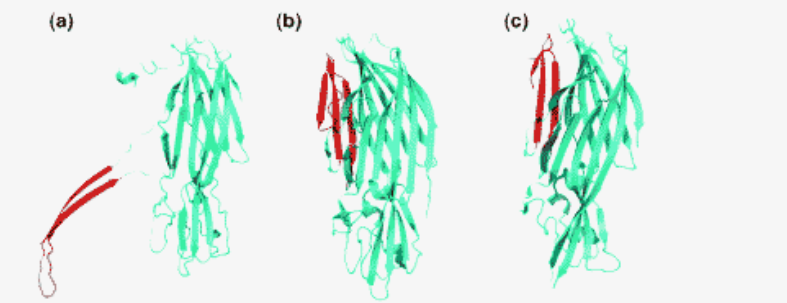

Figure-3: Examples of Three β-Pore Forming Toxins. Shown are the structures of α-HL subunit (A), LukF monomer (B), and LukS monomer (C). The *β*-sheets are represented in green, and the *β*-barrel hairpin loop structures are represented in red. Adapted and modified from: Tilley and Saibil, 2006.

Pore-Forming Toxin of Interest: Cry PFTs

One of the most well studied groups of pore-forming toxins are the cry proteins produced by *Bacillus thuringiensis.* The bacterium *Bacillus thuringiensis (Bt)* was discovered in 1911 by a German scientist named Ernst Berliner who isolated the strain from a dead Mediterranean moth larvae (Ibrahim *et al.*, 2010). About 25 years after its initial discovery, scientists found that the insecticidal activity of Bt was due to its production of paraporal crystal Cry proteins (Ibrahim *et*

al., 2010). In the 1960, Bt was commercially exploited as an insecticide in the U.S.(Ibrahim *et al.*, 2010).

The cry proteins produced by sporulating Bt are a large, diverse group of proteins that have pesticide activity (Palma et al., 2014). A total of 73 types of Cry proteins have been classified so far, and these proteins are known to affect both insects and nematodes (Palma *et al*., 2014). Cry5B attack begins by the ingestion of the toxin subunits by the target, where the Cry toxin dissipates to the intestine where they are activated by proteases (Hui et al., 2012). Upon activation, the protoxin selectively binds to specific receptors located on the target's cell membrane, forms an oligomeric pore, and is inserted into the membrane (Bravo *et al*., 2013). After binding the membrane, pores are formed in the membrane of the intestinal midgut. These pores lead to disruption of the osmotic balance, lysis of the midgut epithelium, and eventually death of the organism (Bravo *et al.*, 2013).

Cry5B: Structure and Mechanism of Infection

Examples of cry proteins produced by sporulating Bt that directly target nematodes are Cry5B and Cry14B. Between Cry5B and Cry14B, Cry5B is the most extensively researched nematicidal Cry protein (Glazer and Nakaido, 2007). (Glazer and Nikiado, 2007). **Figure-4** shows the secondary structure of Cry5b which consists of three domains. The first domain contains 5 helices arranged in an α-helical bundle (Hui *et al*., 2012). This domain is thought to be the determining mechanism for pore formation (Hui *et al*., 2012). Domain-2 is the most structurally divergent domain, and does not closely resemble any other known cry protein domain (Hui *et al*., 2012). Domain-2 is composed of four β-sheets arranged parallel in a β-prism structure, and is thought to be the major contributor for receptor binding (Xu *et al*., 2014). The

structure of the third domain is very similar to the domain-3 structure of other cry proteins, and is thought to be involved in glycolipid receptor recognition (Xu *et al*., 2014).

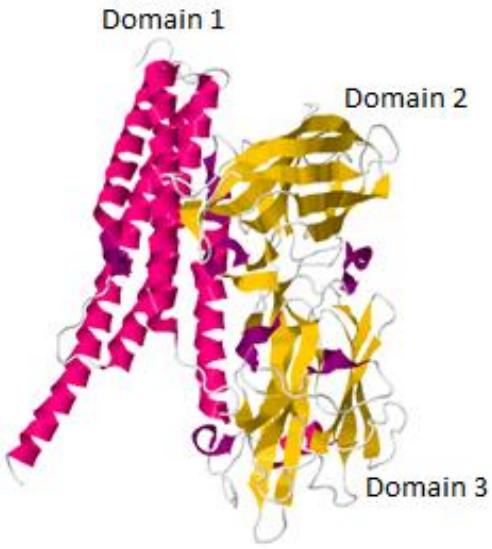

Figure-4: Secondary Structure of Cry5B. This pore-forming toxin consists of 3 domains. Domain-1 contains 5 alpha-helices, domain-2 contains 4 beta-sheets, and domain-3 functions in binding the glycolipid receptor. Adapted from: Hui et al., 2012.

The mechanism of bacterial infection using Cry5B begins by ingestion of the toxin by the nematode (Glazer and Nikaido, 2007). Once ingested, Cry5B dissipates to the intestinal midgut where it is solubilized and activated by proteases to release the protoxin (Hui *et al*., 2012). Cry5B binds to specific glycolipid receptors located on the surface epithelial cells of the intestinal midgut (Glazer and Nikaido, 2007). Binding of the Cry5B toxin to its receptor causes a conformational change of the toxin to allow insertion into the plasma membrane (Hui *et al*., 2012). Insertion of the toxin into the plasma membrane leads to its oligomerization that enhances transmembrane pore formation (Hui *et al*., 2012). The pores allow for influx of sodium ions and water, which eventually leads to lysis of the cells causing severe damage to the intestinal midgut and eventually death of the nematode (Glazer and Nakaido, 2007).

History of the nematode *Caenorhabditis elegans*

Caenorhabditis elegans (C. *elegans*) is a free living saprophytic nematode species found in most temperate regions, which grows to a length of about 1-2 mm when fully developed (Blaxter, 1998). C. *elegans* primarily feeds on bacteria and other microorganisms (Félix and Braendle, 2010). Most nematodes are hermaphrodites, but some males do arise within the population (Félix and Braendle, 2010). The anatomy between both sexes is remarkably similar, but the males are slightly smaller, lack oocytes, and their tail bears a distinctive feature called the copulatory apparatus (Hope, 1999). The anatomy of C. *elegans* is shown in **Figure-5**.

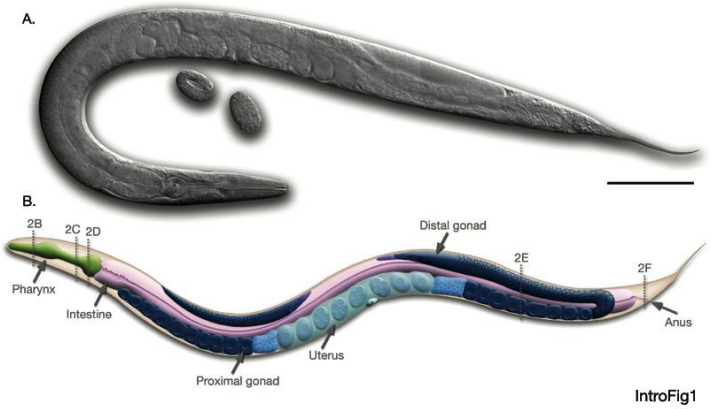

Figure-5: Diagram of C. *elegans* Anatomy. Shown are some of the major distinguishing features of the C. *elegans* including the pharynx, which is composed of about 20 muscle cells, and the large gonads of the organism. Artwork by Altun and Hall, 2005.

C. elegans has a short life cycle which is comprised of three main stages: embryonic development, the larval stage (L1-L4), and adulthood (Corsi, 2006) (**Figure-6**). The overall life span for *C. elegans* is about 2-3 weeks (Hope, 1999). The first stage of the life cycle is embryonic development where the embryo begins to develop inside the hermaphrodite (Corsi, 2006). A single hermaphrodite can lay about 300 eggs, and once laid the eggs typically hatch after 14 hours (Corsi, 2006). After hatching, the larva goes through four molts (L1-L4) (Hope, 1999). During the L1 stage, if environmental conditions are unfavorable (overcrowding or

inefficient nutrients), the larva enter an intermediate growth stage called the daeur phase and can remain in this intermediate stage for several months until conditions become more favorable (Hope, 1999). Once conditions are favorable, the larva exit the dauer phase and enter the L4 stage to eventually become an adult (Hope, 1999).

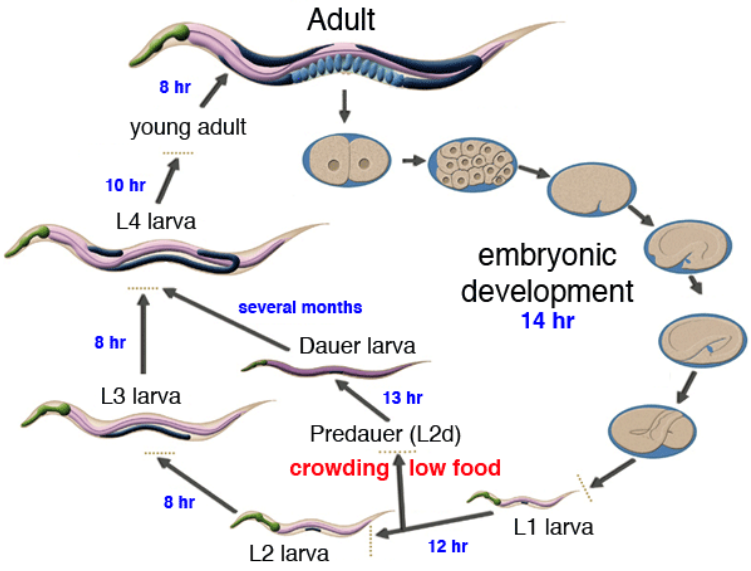

Figure-6: Diagram of the *C. elegans* Life Cycle at 22˚C.
(Artwork by Altun and Hall, 2005)

C. *elegans* as a Model Organism for Toxicology Studies

C. *elegans* is an important organism for scientific research and has become a key biological model for experiments (Boyd *et al*., 2012). Some of the invaluable characteristics of C. *elegans* that have contributed to its success as a model organism include its small size, short lifespan, high cellular complexity, cost-effective cultivation, and genetic manipulability (Kaletta and Hengartner, 2006). C. *elegans* have become increasingly used in toxicology as they share many of the same biological properties as humans (Kaletta and Hengartner, 2006). Studies have found that about "40-75% of human disease-causing genes" identified to date contain homologs within C. *elegans* (McVey *et al*., 2012). This similarity to humans and higher-level organisms

allows scientists to use C. *elegans* as both an *in vivo* and *in vitro* model organism to study complex behaviors and interactions of chemicals with targets in an organism (Leung *et al*., 2008).

Another contributing factor to the increasing use of C. *elegans* as a model for toxicology is the recent advances in microbiology. Because of C. *elegans* cost-effectiveness, the genome of this organism has been intensively studied and has provided researchers with a complete cell lineage map, established genetic methodologies such as RNA interference (RNAi), and many knockout (KO) mutant libraries (Leung *et al*., 2008). Most recently, C. *elegans* has been beneficial for research studies on pesticides; using C. *elegans* as model, scientists are able to study the *in vivo* mechanisms of toxins and predict their effects on other organisms (McVey *et al*., 2012).

C. *elegans* Defense Mechanisms Against Cry5B

The immune system is an interacting network of effector cells and molecules that provide protection against infectious agents. C. *elegans* does not have an adaptive immune system, but does have an innate immune system (Pukkila-Worley and Ausubel, 2012). The nematicidal crystal proteins from the pore-forming toxin Cry5B have been found to target C. *elegans* intestinal epithelial cells (Pukkila-Worley and Ausubel, 2012). High concentrations of Cry5B causes complete midgut cell lysis resulting in *C. elegans* death. But low concentrations of Cry5B stimulate the C. *elegans* innate immune defense mechanisms (Pukkila-Worley and Ausubel, 2012). Intoxication of C. *elegans* by Cry5B is phenotypically easy to observe, as intoxicated worms appear lethargic, pale in coloration, and small in size (Pukkila-Worley and Ausubel, 2012). The toxic effects of Cry5B also cause worms to have a lack of pumping,

reduction in fertilized eggs, developmental delay, and increased mortality compared to wild type, normal C. *elegans* (Kao *et al*., 2011).

Several innate defense pathways are used by C. *elegans* as protection against Cry5B (**Figure-7**), including the AP-1/JNK MAPK pathway (diagram left side), NSY-1/SEK-1/PMK-1 MAP kinase pathway which is analogous to the p38/MAPK pathway (diagram middle), and the Rab-5/Rab-11 pathway (diagram right side) (Los *et al*., 2011). Each of these pathways is discussed below in more detail.

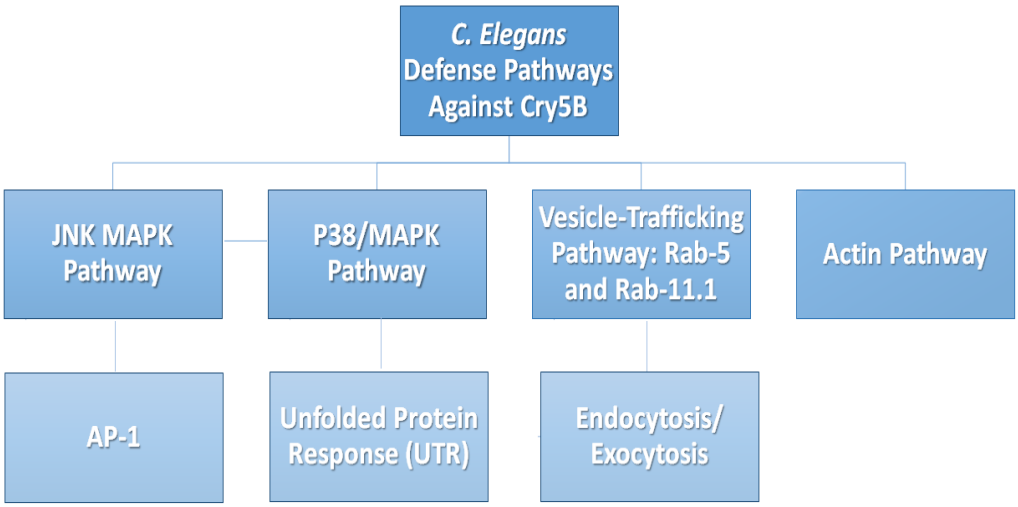

Figure-7: Summary of C. *elegans* Defense Pathways Against Cry5B Toxin. Modified and Adapted from Los *et al.*, 2011. Three main innate immune pathways are used by C. elegans against Cry5B including from left to right: the JNK/MAPK/AP-1 pathway, p38/MAPK pathway, and the Rab-5/11.1 pathway. The fourth pathway is the actin pathway which the Aroian's data has shown provides defense.

p38/MAPK Pathway

The p38/MAPK pathway was the first defense pathway providing protection against PFTs that was discovered in C. *elegans* (Los *et al*., 2011). The mitogen-activated protein kinases (MAPK) are highly-conserved protein kinases that function to phosphorylate and activate transcription factors that control signal transduction pathways (Los *et al*., 2011). This pathway

coordinates defense in the C. *elegans* against a wide range of pathogenic bacteria. An important downstream target of the p38/MAPK pathway is the unfolded protein response (UPR) pathway (Los *et al*., 2011) that helps to refold misfolded proteins in the ER. The upregulation of UPR genes is a protective survival response against Cry5B toxins as it monitors and maintains the protein-folding condition in the endoplasmic reticulum (Los *et al*., 2011).

AP-1/JNK MAPK Pathway

The AP-1/Jun (JNK) MAPK pathway is another defense pathway that stimulates resistance against Cry5B. JNK is responsible for activation of the MAPK p38 pathway which is important in production of inflammatory mediators (Los *et al*., 2011). The JNK MAPK pathway was found to be a "key regulator of PFT defense," and the downstream target of this pathway AP-1 is required for defense against PFTs (Los *et al*., 2011).

Rab-5/Rab-11.1 Vesicle-Trafficking Pathway

The third innate pathway involved in resistance to PFTs is a vesicle-trafficking pathway that involves endocytosis and exocytosis in the plasma membrane (Kao *et al*., 2011). Membrane trafficking is important as it mediates the transport of proteins and other macromolecules within the Golgi body to the plasma membrane (Kao *et al*., 2011). Two key Rab proteins: Rab-5 and Rab-11 were found to regulate both endocytosis and exocytosis in the plasma membrane, and are vital for pore-forming toxin defense because vesicles help repair pore damage to the plasma membrane (Kao *et al*., 2011).

Actin Pathway

The actin pathway is thought to be a distinct pathway that provides defense against PFT attack. Actin plays a critical role throughout the life of *C. elegans*. It is important for both early development as well as intestinal defense (Hupp *et al*., 2013). The apical layer epithelial cells in the intestine are composed of actin and intermediate filaments (Hupp et al., 2013). The actin cytoskeleton functions in defense processes and cell motility, making it a key target for cry toxins (Hupp *et al*., 2013). Pore-forming toxins have been found to interact with actin both directly and indirectly (Hupp *et al*., 2013). Direct interaction causes a re-localization of actin from the apical surface of the intestine to the basolateral side, which causes gap formation in the intestinal lumen (Hupp *et al*., 2013). PFTs also indirectly induce actin to promote protoxin uptake by endocytosis (Vega-Cabrera *et al*., 2014). The Aroian lab has previously found that the actin-related gene nck-1, including the Arp2/3 complex, is important for Cry5B defense (Sitaram, unpublished data). Their data supports the hypothesis that nck-1 and the Arp2/3 complex defense pathway are distinct from the known sek-1/MAPK defense pathway (Sitaram, unpublished data). Studies have found that when actin genes are silenced, worms show increased hypersensitivity to Cry toxins, thus supporting the hypothesis that actin is important for specific defense mechanisms in *C. elegans* (Vega-Cabrera *et al*., 2014). Whether actin defense is a distinct defense pathway, or works along with the other known innate pathways is still unknown.

Genes of Interest: Erm-1, Dbn-1, Plst-1, F38E9.5

Four actin-interacting genes were chosen from the Aroian lab's list of genes upregulated by *C. elegans* in response to Cry5B, and were tested in this project for knockdown in using RNA

interference (RNAi) to determine their role in Cry5B defense. The four actin related genes chosen are: Erm-1, Dbn-1, Plst-1, and F38E9.5.

Erm-1 (Ezrin/Radixin/Moesin-1) as defined by WormBase is a family member of cytoskeleton linkers used to connect the plasma membrane to cytoskeletal elements such as actin filaments, microtubules, and intermediate filaments. Full RNAi knockdown of Erm-1 in *C. elegans* has proved to be lethal; Erm-1 is essential for normal embryonic development of the intestine (McGhee, 2007).

DreBriN-1 (Developmentally REgulated BRaIN protein) (Dbn-1) as defined by WormBase is an ortholog of human DBN1, and is predicted to participate in actin-binding and bundling activity. Dbn-1 has been found to be a target of the p38 MAPK pathway during the formation of muscle tissue in embryonic development (Butkevich *et al*., 2015). Similar to Erm-1, full RNAi knockdown of Dbn-1 is lethal, as Dbn-1 is vital for muscular development.

The third gene tested in this project by knockdown using RNAi was the (PLaSTin (actin bundling protein) homolog (Plst-1) gene which is an ortholog of human PLS1. Plst-1 is defined by WormBase as an actin-bundling protein required during embryonic development.

The final gene studied in this project was F38E9.5, defined by WormBase as an ortholog of human twinfilin actin-binding protein TWF1 and TWF2. It is expressed in muscle as well as the nervous system.

PROJECT PURPOSE

Through a proteomics approach, the Aroian lab at UMMS has identified a list of proteins (and their associated genes) whose levels changed significantly when *C. elegans* were fed Cry5B toxin. From this list, the most noticeable changes were seen for proteins that interact with actin. The Aroian lab has previously found that the actin-related gene nck-1, including the Arp2/3 complex, is important for Cry5B defense (Sitaram, unpublished data). Their data supports the hypothesis that the nck-1/Arp2/3 defense pathway is distinct from the sek-1/MAPK pathway (Sitaram, unpublished data). The purpose of this MQP was to test the hypothesis that PFT defense depends on controlling actin. Four actin-interacting proteins (DBN-1, ERM-1, PLST-1 and F38E9.5) were tested to see if these proteins had an important function for Cry5B toxin defense and repair in *C. elegans*. To test this hypothesis, these proteins were knocked down, and the affected worms were analyzed for toxin hypersensitivity, alterations in pore repair and endocytosis capability, and for interactions of these proteins with other previously-described defense pathways.

METHODS

C. *elegans* Strains

All *C. elegans* strains were maintained at 20°C and cared for using standard conditions and techniques (Brenner, 1974). Strains used were wild-type Bristol strain N2, nck-1 (ok694), *pgp-1::gfp*, rab-11.1, sek-1 (km4), VP303 rde-1(ne219); kbEx200 [rol-6(su1006)]. All *C. elegan*s strains were provided by the Aroian lab.

Microscopy

C. elegans were pipetted on 2% agarose pads containing a 1:100 dilution of 1.5 mM sodium azide. Worms were photographed under the 40X objective using a confocal microscope.

RNA interference (RNAi), Dilutions, and Plates

The tested *C. elegans* strains were allowed to feed on the RNAi plates for ~ 24 hours. Interference (RNAi) bacteria rab-11.1, dbn-1, and erm-1 were diluted in empty vector (pL4440) control bacteria to provide synchronous L4 development. Rab-11.1 was diluted by 1/6 with pL4440 control bacteria. Act-5, arx-5, dbn-1, eps-8, and erm-1 were diluted by 50% with pL4440 control bacteria. F38E9.5, L4440, nck-1, plst-1, sek-1, were not diluted during any of the experiments. To make RNAi plates, frozen stocks of RNAi bacteria transgenically expressed by *E. coli* were streaked onto LB AMP plates and grown overnight at 30°C. The following day, the RNAi bacteria were inoculated and cultured overnight at 30°C. The overnight cultures were diluted with LB so that the ENGIA plates contained mid-log phase RNAi bacteria with an optical density of ~3 at OD_{600}.The lawns were grown overnight at 25°C and the plates were used within

1 day. For each experiment requiring RNAi plates, synchronous L1 worms were plated onto the lawns.

Cry5B toxin plates

Cry5B toxin plates were prepared by streaking frozen stocks of the *E. coli* strain JM103 carrying the empty vector pQE9, and the *E. coli* strain carrying the Cry5B gene onto ENG plates, and incubated overnight at 30°C. The following day, the empty vector and the strain carrying the Cry5B gene were inoculated and cultured overnight at 30°C. The overnight cultures were diluted 1:10 in fresh LB media and grown for 1 hour shaking at 30°C. After 1 hour, the cultures were induced with 1mM isopropyl β-d-thiogalactoside (IPTG) at 30°C. After induction, the cultures were allowed to grow for an additional 3 hours at 37°C. For 2% and 5% Cry5B plates, the Cry5B culture was diluted with the empty vector. Cry5B plates were made by spreading 50µl of bacteria with an optical density of ~2 at OD_{600} on p100 ENGIA plates. The lawns were grown overnight at 25°C and the plates were used within 1 day. For each experiment requiring Cry5B plates synchronous L4 worms were manually picked or plated onto the lawns.

Hypersensitivity Assay

Synchronized VP303 L1 larvae were plated on RNAi plates and grown to the L4 stage (~52 hours). Once the animals reached the L4 stage while feeding on the RNAi plates, 10 animals were manually picked to the 0% and 2% Cry5B toxin plates. After 48 hours, the worms were picked to a 9 well glass plate containing 1.5 mM of sodium azide diluted in M9 and photographed.

Pore Repair Assay

Synchronized N2 L1 larvae were plated on RNAi plates and grown to the L4 stage, then transferred to 100% Cry5B plates for 1 hour. After 1 hour, half of the worms were transferred to recovery plates and the other half were transferred to microfuge tubes containing serotonin and 6.7 μg/mL propidium iodide (PI) to shake for 45 minutes. After 45 minutes, the worms were transferred to 2% agarose slides and a total of 50 worms were scored for leakage of the ingested PI into the cytosol of intestinal epithelial cells. The dye feeding and analysis was performed on the worms on the recovery plates 24 hours later.

Gene Interacting Assays: Sek-1 (km4) and Nck-1 (ok694) LC50 Assays

Synchronized sek-1 (km4) or nck-1(ok694) L1 larvae were plated onto RNAi plates to feed and grow to the L4 stage (~46 hours) at 20°C. RNAi bacteria was induced by 1mM IPTG for 1hr at 37°C while shaking. The LC50 survival assays were set up and scored based on the published protocol (Los, *et al.*, 2011). Changes made to the procedure were to the Cry5B concentrations as 5μl of 3 fold diluted, purified Cry5B, or the control ("Hepes pH 8.0 to a concentration of 0.5mM") was added to the respective wells (Los, *et al.*, 2011). The same exact procedure was repeated for the nck-1 (ok694) strain. Worms were scored as dead if there was no movement after prodding the animal three times with an eyelash pick.

Endocytosis Assay

Synchronized pgp-1::gfp L1 larvae were plated on RNAi plates and grown to the L4 stage (~57 hours) at 20°C before being transferred to 100% Cry5B toxin plates and fed for 2 hours. After Cry5B feeding, the animals were transferred to 2% agarose slides and photographed

at 40X using a confocal microscope to visualize GFP+ endocytic vesicles induced by toxin exposure.

Statistical Analysis

All statistical analysis was performed using Excel. The data from the Pore Repair Assay and gene interacting assays were analyzed with error bars representing mean s.e.m.; ANOVA followed by Student's t-test; n=3 per each sample ;*p<0.05; **p<0.01; *** p<.001. The gene interacting assays (worm survival curves): *sek-1(km4)* and *nck-1(ok694)* LC50 assays were analyzed with error bars representing mean s.e.m.

To quantitatively determine the amount of vesicle formation seen for each tested RNAi condition in the endocytosis assay the following constraints were created. Using florescent microscopy, 20 single worms from each RNAi condition were randomly imaged at two different channels. The first channel was the green channel to view the fluorescing GPF tagged vesicles and the natural fluorescing gut granules. The second field used the blue channel to view the natural fluorescing gut granules. From the photographs the 3 highest quality pictures in the blue and green channel for each RNAi condition were selected. A high quality photograph was defined as a picture containing a single worm where the major structural features could be clearly distinguished. For each photograph taken in the green channel, the number of green fluorescing spots seen were counted. A "fluorescing spot" is defined as a glowing single, distinct, circular fluorescing spot located outside the apical surface of the intestine. Fluorescing spots that overlapped and could not be clearly distinguished from each other were counted as one fluorescing spot. Fluorescing spots that were hard to distinguish were ignored. This method was repeated for the three photographs of the single worm for each RNAi condition. The number of florescent spot and gut granules were averaged to determine the percent of vesicle formation for each RNAi condition.

RESULTS

The Aroian lab previously identified several proteins that were differentially regulated when *C. elegans* were fed the toxin Cry5B. From this list, the proteins whose levels changed significantly were the actin-regulating proteins. I selected several knockdown genes from the set of actin-interacting proteins that were differentially regulated for further experimentation by gene knockdowns.

Hypersensitivity Assay

A hypersensitivity assay using Vp303 mutants was used to screen six selected knockdown genes from the set of actin-associated proteins that were differentially regulated by Cry5B. *C. elegans* VP303 strain was used as this strain performs RNAi only in the intestine. The genes that were tested were empty vector (L4440 WT control), Nck-1 (positive control), Sek-1 (positive control), 50% Arx-5 (part of Arp 2/3 complex), 50% dbn-1, 50% eps-8 (intestinal morphogenesis), 50% erm-1, 50% dbn-1, plst-1, and F38E9.5. After 48 hours of feeding on 0% and 2% Cry5B toxin plates, the worms were photographed (**Figure-8**). Intoxication by Cry5B is phenotypically easy to observe, as intoxicated worms appear pale in coloration and small in size. The knockdown of four genes (dbn-1 (e), erm-1 (g), plst-1 (h), and F38E9.5 (i)), led to altered sensitivity to subsequent feeding of Cry5B compared to empty vector, and these four genes were selected for further experimentation. Dbn-1, erm-1 and plst-1 showed increased hypersensitivity to intoxication of Cry5B, as these RNAi worms appeared pale almost clear in coloration, showed a clear decrease in size, and most of the worms were dead on the plate compared to WT worms. F38E9.5 worms appeared slightly healthier in comparison to WT, as these worms were robust in color and did not show a decrease in size.

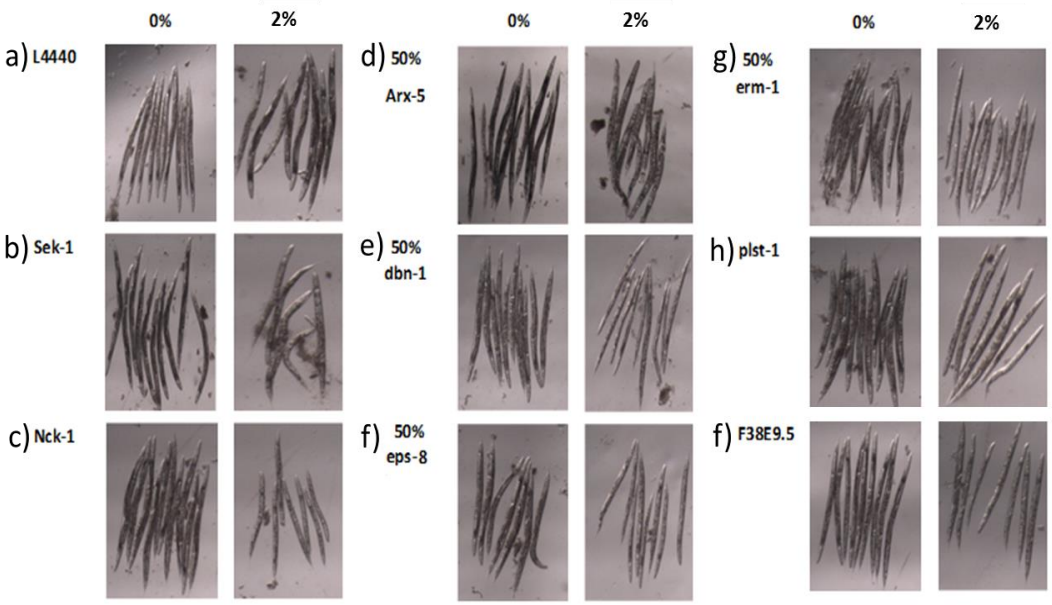

Figure-8: Cry5B Hypersensitivity Assay Following Intestinal RNAi. The knockdown of four genes (dbn-1 (e), erm-1 (g), plst-1 (h), and F38E9.5 (i)), led to altered sensitivity to subsequent feeding of Cry5B compared to empty vector, and were selected for further experimentation.

Pore Repair Assay

A pore repair assay using N2 (Bristol wild type worms) was performed to determine whether the selected proteins DBN-1, ERM-1, PLST-1, and F38E9.5 have a functional role in pore repair and maintenance. RNAi fed N2 L4s were pulsed on 100% Cry5B toxin plates for 1 hour and were scored by microscopy for percent leakage immediately or after 24 hours. Worms with pore damage show leakage of ingested propidium iodide into the cytosol of intestinal epithelial cells. Microscopy was used to score fifty worms from each RNAi condition based on whether leakage or no leakage was seen in the intestine of the worm. Photographs (Appendix A, **Figure-1**) depicting normal vs. leakage due to pore damage for each RNAi strain were also taken. The data from the pore-repair assay was plotted on a graph. RNAi of actin-associated proteins DBN-1 and ERM-1 (**Figure-9**) led to a significant reduction of pore repair abilities.

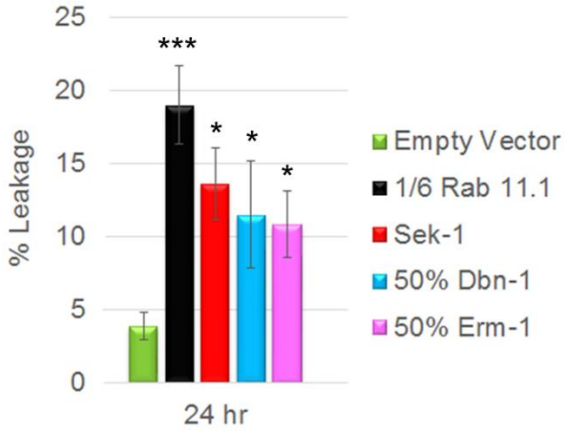

Figure-9: Pore Repair Assay: Percent of Leakage in the Cytoplasm of Intestinal Cells after 1 Hr Cry5B Intoxication Testing RNAi DBN-1 and ERM-1. After 24 hours of recovery the worms with DBN-1 and ERM-1 RNAi show a significant reduction in pore repair abilities compared to empty vector worms. Mean± s.e.m.;*p<0.05; **p<0.01; *** p<.001; ANOVA followed by Student's t-test; n=3 per each sample.

The pore repair assay was repeated **(Figure-10)** using RNAi for PLST-1 (blue histobar) and F38E9.5 (yellow histobar). Knockdown of these proteins did not show any significant difference in pore repair ability compared to the control. This data suggests that both PLST-1 and F38E9.5 do not regulate pore repair maintenance.

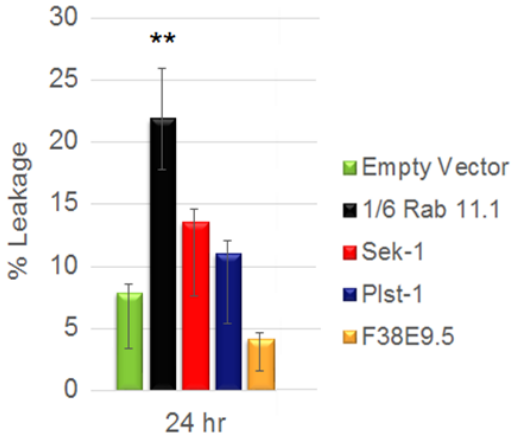

Figure-10: Percent of Leakage in the Cytoplasm of Intestinal Cells after 1 Hr Cry5B Intoxication Testing RNAi PLST-1 and F38E9.5. After 24 hours of recovery the worms with PLST-1 and F38E9.5 RNAi did not be required for pore-repair mechanisms. Mean s.e.m.;*p<0.05; **p<0.01; *** p<.001; ANOVA followed by Student's t-test; n=2 per each sample.

Endocytosis Assay

One of the known *C. elegans* defense mechanisms against PFTs is vesicle formation. This defense mechanism causes re-localization of the apical plasma membrane to the pore structures as a response to damage by Cry toxins (Los *et al.*, 2011). An endocytosis assay using a PGP-1::GFP strain was used to study whether DBN-1, ERM-1, PLST-1, and F38E9.5 directly provide Cry5B toxin defense in the plasma membrane of *C. elegans*. PGP-1::GFP localizes strictly to the apical membrane of the intestinal cells which allowed the *in vivo* effects of Cry5B to be seen using confocal microscopy (Los *et al.*, 2011). A total of seven RNAi proteins: empty vector (control), SEK-1 (negative control), RAB 11.1 (positive control), DBN-1, ERM-1, PLST-1, and F38E9.5 were tested. Photographs of vesicle formation were taken of the nematodes for each RNAi condition to visualize the GFP+ endocytic vesicles induced by toxin exposure (**Appendix A**, **Figure-2**). The percent of vesicle formation was determined using the constraints outlined in the methods. Knockdown of actin-associated proteins DBN-1 and ERM-1 showed a decrease in vesicle formation compared to the empty vector control, suggesting that these two proteins are important for vesicle formation defense (**Table-1**). The actin-interacting proteins PLST-1 and F38E9.5 showed a high percentage of vesicle formation that was similar to the empty vector control (**Table-1**). These results suggest that PLST-1 and F38E9.5 do not provide PFT protection by vesicle formation (**Table-1**).

Table 1- Percent of Vesicle Formation

RNAi	Average # of florescent spots	Average # of gut granules	% Vesicle Formation
Empty Vector	96	34	65%
Sek-1	123	38	69%
Rab 11.1	73	60	18%
Dbn-1	125	74	41%
Erm-1	88	59	33%
Plst-1	204	73	64%
F38E9.5	140	58	59%

The average represents a mean of florescent spots or gut granules counted for triplicate photograph sets. A "florescent spot" is defined as GFP fluorescing vesicles and gut granules.

Gene Interacting Assays (LC50 Assays)

Sek-1 (*Km4*) and Nck-1 (*Ok694*) LC50 assays were performed to quantitatively determine whether the actin-associated genes of interest DBN-1, ERM-1, PLST-1, and F38E9.5 function in one of the known MAPK pathways, or work in a different defense pathway. LC50 assays are quantitative, dose-dependent lethality assays used to determine the concentration of Cry5B that is lethal to 50% of the tested animals (Los, *et al.,* 2011).

Sek-1 (km4) LC50 Assays

The sek-1 (*km4*) gene is known to function within the p38/MAPK defense pathway against Cry5B. The LC50 assays (**Figure-11**) were scored after six days by counting the survival of the worms for each RNAi condition. Worms were scored as dead if there was no movement after prodding the animal three times with an eyelash pick. NCK-1 was used as a positive control, as the Aroian lab has previously discovered that the nck-1 (*ok694*) defense pathway is distinct from the sek-1/p38/MAPK pathway (Sitaram, unpublished data). The results showed that RNAi DBN-1 and ERM-1 (pink curve) expressed increased hypersensitivity to Cry5B toxin

compared to the empty vector control (green curve). This suggests that actin-interacting proteins DBN-1 and ERM-1 function in a defense pathway that is distinct from the known p38 MAPK pathway.

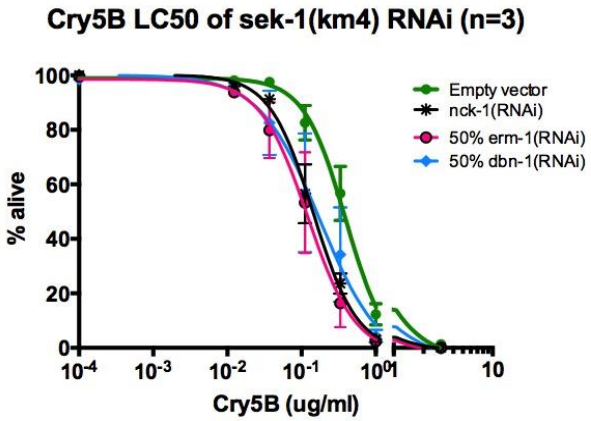

Figure-11: Sek-1 (*km4*) LC50 Assay Cry5B Dose Response Curve with RNAi DBN-1 and ERM-1. The concentrations of Cry5B are plotted on a logarithmic scale. Plotted data are the mean ± s.e.m. of 3 trials.

The results of the sek-1 (*km4*) LC50 assay for the PLST-1 and F38E9.5 actin-associated genes (**Figure-12**) suggest that PLST-1 functions in a defense pathway that is distinct from the p38 MAPK pathway, as the curve shows that knockdown of PLST-1 (blue curve) caused worms to have increased sensitivity to Cry5B toxin compared to empty vector (green curve). Conversely, the results for F38E9.5 (yellow curve) showed that worms containing F38E9.5 RNAi showed *increased* survival compared to empty vector (green curve). This suggests that F38E9.5 may function in a pathway that is distinct from the known p38/MAPK pathway and the actin pathway.

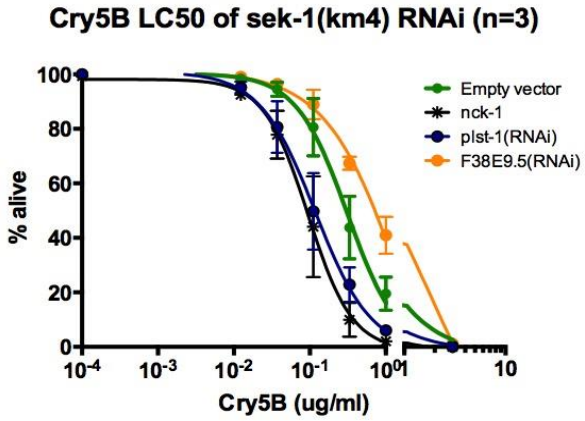

Figure-12: Sek-1 (*km4*) LC50 Assay Cry5B Dose Response Curve Testing RNAi PLST-1 and F38E9.5. The concentrations of Cry5B are plotted on a logarithmic scale. Plotted data are the mean± s.e.m. of 3 trials.

Nck-1 (ok694) LC50 Assay

The Aroian lab previously determined that gene nck-1 (*ok694*) which is involved in actin dynamics, functions in a defense pathway that is distinct from the sek-1/p38/MAPK pathway (Sitaram, unpublished data). The nck-1 (ok694) LC50 well assay (**Figure-13**) was used to determine whether actin-interacting genes dbn-1 and erm-1 were distinct from the nck-1/apr2/3 actin defense pathway. The percent survival averages for each tested RNAi condition, were plotted on a logarithmic scale. The results show that DBN-1 (pink curve) and ERM-1 (blue curve) RNAi animals had similar hypersensitivity to Cry5B relative to the empty vector control animals (green curve). This suggests that DBN-1 and ERM-1 function in the same defense pathway as the actin-related gene nck-1.

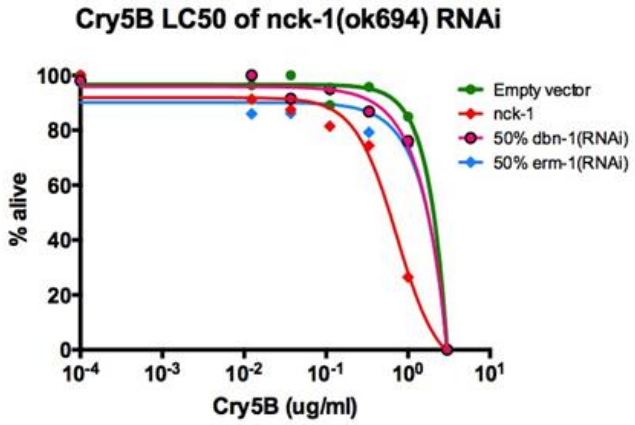

Figure-13: Nck-1 (ok694) Dose Response Survival Curve. The concentration of Cry5B are plotted on a logarithmic scale. This graph represents N=1. Each line is representative of the percent alive averages from three wells that were scored for each of the seven Cry5B concentrations.

The results in **Figure-14** show a comparison of 5 gene knockdowns using a distinguishing Cry5B concentration which produced the most notable change in percent survival for each RNAi condition (10^{-1} µg/mL of Cry5B toxin). The nck-1(*ok694*) LC50 assay was repeated to N=3 using the 10^{-1} µg/mL of Cry5B concentration. The results support the sek-1 survival curve data that DBN-1 and ERM-1 function in a pathway distinct from the known MAPK defense pathway, and function in a pathway similar to the nck-1/arp2/3 complex actin pathway.

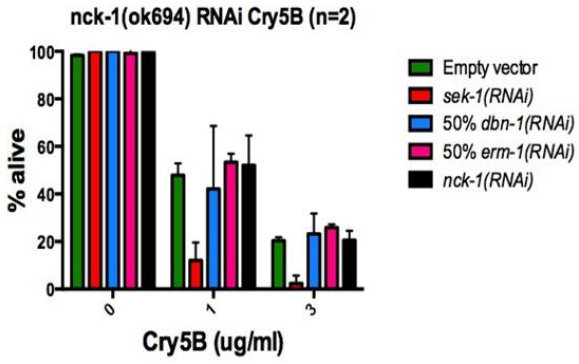

Figure-14. Comparison of 5 Gene Knockdowns at a single Cry5B Concentration of 0.1 µg/ml. Nck-1 (*ok694*) LC50 Assay Cry5B Response at 10^{-1} testing DBN-1 and ERM-1. Mean ± s.e.m.

DISCUSSION

Pore-forming toxins are the most commonly secreted bacterial exotoxins and are often pathogenic bacteria's main mode of virulence (Menestrina *et al*., 2011). Through evolution, cells have developed specific defense mechanisms to offer protection against plasma membrane perforation by PFTs (Los *et al*., 2011). The purpose of this MQP was to test the hypothesis that *C. elegans* pore-forming toxin defense against ingested Cry5B is dependent on the regulation of actin. To test this hypothesis four actin-interacting proteins (DBN-1, ERM-1, PLST-1 and F38E9.5) were knocked down and the affected worms were analyzed for toxin hypersensitivity, alterations in pore repair and endocytosis capability, and for interactions of these proteins with other previously-described defense pathways.

Previous research has found that actin may act in a distinct defense pathway that provides defense against PFT attack. These studies found that when actin genes are silenced, affected worms show increased hypersensitivity to PFT (Vega-Cabrera *et al*., 2014). Taken together, the data presented in this project suggests that actin-interacting proteins DBN-1, ERM-1, and PLST-1 are important for survival against PFT attack. Specifically, this data correlates that acting interacting proteins DBN-1 and ERM-1 are important for intestinal plasma membrane pore repair and are responsible for inducing the vesicle trafficking pathway after attack by Cry5B (**Figure-9** and **Table-1**). The results also suggest that actin-related protein PLST-1 is important for survival after Cry5B toxin attack as this protein showed increased hypersensitivity compared to empty vector in the VP303 Cry5B hypersensitivity assay (**Figure-8**). The *sek-1(km4)* LC50 assay data and the *nck-1(ok694)* LC50 data are consistent with the Aroian's previous research which found that actin-related gene nck-1, including the arp2/3 complex, are important for Cry5B defense (Sitaram, unpublished data). The *sek-1(km4)* LC50 assay data suggest that DBN-1, ERM-1, and

PLST-1 actin-associated proteins function in a pathway distinct from the known sek-1/MAPK pathway (**Figure-11 and Figure-12**). The *nck-1(ok694)* LC50 data (**Figure-13**) provided support for a model in which DBN-1 and ERM-1 work together with NCK-1, which is also known to modulate actin. These results provide further support to the Aroian's hypothesis that the nck-1 and the Arp2/3 complex defense pathway are distinct from the known sek-1/MAPK defense pathway (Sitaram, unpublished data). Conversely, the data for RNAi of actin-regulated protein F38E9.5 suggest that when this protein is knocked down the worms have increased protection to Cry5B. The F38E9.5 knockdown in the VP303 Cry5B hypersensitivity assay (**Figure-8**) phenotypically appeared more protected when exposed to Cry5B compared to WT. The *sek-1(km4)* LC50 assay (**Figure-12**) results for F38E9.5 show that MAPK-null mutants appear to have increased protection from Cry5B; suggesting that this protein may work in a defense pathway that is both distinct from the sek-1/MAPK pathway as well as the nck-1/arp2/3 complex pathway.

Problems that occurred during this project included for the pore repair assay, not showing the data for percent leakage when the worms were immediately exposed to toxin, as the results were concluded to be unsubstantial. This data was removed due to the low number of worms that ingested the propidium iodide. Apart from this, no other major problems occurred during this research.

In summary, this study suggests that loss of one of these key actin interacting proteins DBN-1, ERM-1, and PLST-1 results in increased hypersensitivity to the PFT toxin Cry5B, as well as loss of cellular protection. This study extends previous findings in our lab, and offers more insight into the cellular defense mechanisms against PFT attack. Further studies should be conducted to determine the exact role of actin in PFT defense and identify the defense pathway being used. Further implications of this study is that understanding cellular defenses toward

PFTs could lead to the development of therapeutic approaches that improve the outcomes of infections and diseases resulting from PFTs (Los *et al*., 2011). Some of the most problematic, pathogenic such as MRSA, *Vibrio cholerae*, and *Streptococcus pneumoniae* employ PFTs as their mode of infection (Los *et al*., 2011). The development of potential drugs that could offer PFT protection in the host by utilizing cellular pathways to prevent tissue damage would be extremely beneficial.

BIBLIOGRAPHY

Altun ZF, & Hall DH (2005) Handbook of *C. elegans* Anatomy. WormAtlas. http://www. wormatlas. org/handbook/contents. htm.

Blaxter M (1998) *Caenorhabditis elegans* is a nematode. *Science*, 282(5396), 2041-2046.

Boyd WA, Smith MV, & Freedman JH (2012) Caenorhabditis elegans as a model in developmental toxicology. *Developmental Toxicology: Methods and Protocols*, 15-24.

Bravo A, Gómez I, Porta H, García-Gómez BI, Rodriguez-Almazan C, Pardo L, & Soberón M (2013) Evolution of Bacillus thuringiensis Cry toxins insecticidal activity. Microbial biotechnology, 6(1): 17-26.

Brenner, Sydney. "The genetics of Caenorhabditis elegans." Genetics 77.1 (1974): 71-94.

Butkevich E, Bodensiek K, Fakhri N, von Roden K, Schaap IA, Majoul I, Schmidt CF, Klopfenstein DR (2015) Drebrin-like protein DBN-1 is a sarcomere component that stabilizes actin filaments during muscle contraction. *Nature Communications*, 2015 Jul 6; 6: 7523. doi: 10.1038/ncomms8523.

Corsi AK (2006) A biochemist's guide to *C. elegans*. *Analytical Biochemistry*, 359(1): 1.

Dal Peraro M, & van der Goot FG (2016) Pore-forming toxins: ancient, but never really out of fashion. *Nature Reviews Microbiology*, 14(2): 77-92.

Félix M-A, & Braendle C (2010) The natural history of *Caenorhabditis elegans*. *Current Biology*, 20(22): R965-R969.

Geny B, & Popoff MR (2006) Bacterial protein toxins and lipids: pore formation or toxin entry into cells. *Biology of the Cell*: 98(11): 667-678.

Glazer AN, & Nikaido H (2007) Microbial biotechnology: fundamentals of applied microbiology: Cambridge University Press.

Gonzalez MR, Bischofberger M, Pernot L, Van Der Goot FG, & Freche B (2008) Bacterial pore-forming toxins: the (w)hole story? *Cellular and Molecular Life Sciences*, 65(3): 493-507.

Heuck AP, & Johnson AE (2005) Membrane recognition and pore formation by bacterial pore-forming toxins. Protein-lipid interactions. From membrane domains to cellular networks, 165-188.

Hope IA (1999) Background on *Caenorhabditis elegans*. *C. elegans* a practical approach, 1-15.

Howard SP, Garland WJ, Green MJ, & Buckley JT (1987) Nucleotide sequence of the gene for the hole-forming toxin aerolysin of *Aeromonas hydrophila*. *Journal of Bacteriology*, 169(6): 2869-2871.

Hui F, Scheib U, Hu Y, Sommer RJ, Aroian RV, & Ghosh P (2012) Structure and glycolipid binding properties of the nematicidal protein Cry5B. *Biochemistry*, 51(49): 9911-9921.

Hupp S, Förtsch C, Wippel C, Ma J, Mitchell TJ, & Iliev AI (2013) Direct transmembrane interaction between actin and the pore-competent, cholesterol-dependent cytolysin pneumolysin. *Journal of Molecular Biology*, 425(3): 636-646.

Iacovache I, Paumard P, Scheib H, Lesieur C, Sakai N, Matile S, Parker M & Van der Goot FG (2006) A rivet model for channel formation by aerolysin-like pore-forming toxins. The EMBO journal, 25(3): 457-466.

Jones KE, Patel NG, Levy MA, Storeygard A, Balk D, Gittleman JL, & Daszak P (2008) Global trends in emerging infectious diseases. *Nature*, 451(7181): 990-993.

Ibrahim MA, Griko N, Junker M, & Bulla LA (2010) Bacillus thuringiensis: a genomics and proteomics perspective. Bioengineered bugs, 1(1): 31-50.

Kaletta T, & Hengartner MO (2006) Finding function in novel targets: *C. elegans* as a model organism. *Nature Reviews Drug Discovery*, 5(5): 387-399.

Kao CY, Los FC, Huffman DL, Wachi S, Kloft N, Husmann M, Karabrahimi V, Schwartz JL, Bellier A, Ha C, Sagong Y, Fan H, Ghosh P, Hsieh M, Hsu CS, Chen L, Aroian RV (2011) Global functional analyses of cellular responses to pore-forming toxins. PLoS Pathog, 7(3), e1001314.

Ladant D, Alouf JE, & Popoff MR (2005) The comprehensive sourcebook of bacterial protein toxins: Academic Press.

Leung MCK, Williams PL, Benedetto A, Au C, Helmcke KJ, Aschner M, & Meyer JN (2008) *Caenorhabditis elegans*: an emerging model in biomedical and environmental toxicology. *Toxicological Sciences*, 106(1): 5-28.

Los FCO, Kao C-Y, Smitham J, McDonald KL, Ha C, Peixoto CA, & Aroian RV (2011) RAB-5-and RAB-11-dependent vesicle-trafficking pathways are required for plasma membrane repair after attack by bacterial pore-forming toxin. *Cell Host & Microbe*, 9(2): 147-157.

Menestrina, G., Dalla Serra, M., & Prévost, G. (2001). Mode of action of β-barrel pore-forming toxins of the staphylococcal α-hemolysin family. *Toxicon, 39*(11), 1661-1672.

McGhee JD (2007) The C. elegans intestine. WormBook 1–36. http://www.wormbook.org/chapters/www_intestine/intestine.html (2007)

McVey KA, Mink JA, Snapp IB, Timberlake WS, Todt CE, Negga R, & Fitsanakis VA (2012) *Caenorhabditis elegans*: An emerging model system for pesticide neurotoxicity. *Journal of Environmental & Analytical Toxicology*, 2012.

Palma L, Muñoz D, Berry C, Murillo J, & Caballero P (2014) Bacillus thuringiensis toxins: an overview of their biocidal activity. Toxins, 6(12): 3296-3325.

Parker MW, & Feil SC (2005) Pore-forming protein toxins: from structure to function. *Progress in Biophysics and Molecular Biology*, 88(1): 91-142.

Pukkila-Worley R, & Ausubel FM (2012) Immune defense mechanisms in the *Caenorhabditis elegans* intestinal epithelium. *Current Opinion in Immunology*, 24(1): 3-9.

Strange, K. (2006). C. elegans: methods and applications (Vol. 351). Springer Science & Business Media.

Tilley SJ, & Saibil HR (2006) The mechanism of pore formation by bacterial toxins. *Current Opinion in Structural Biology*, 16(2): 230-236.
Torsvik V, Øvreås L, & Thingstad TF (2002) Prokaryotic diversity--magnitude, dynamics, and controlling factors. *Science*, 296(5570): 1064-1066.

Vega-Cabrera A, Cancino-Rodezno A, Porta H, & Pardo-Lopez L (2014) Aedes aegypti Mos20 Cells Internalizes Cry Toxins by Endocytosis, and Actin Has a Role in the Defense against Cry11Aa Toxin. *Toxins*, 6(2): 464-487.

Xu C, Wang B-C, Yu Z, & Sun M (2014) Structural insights into *Bacillus thuringiensis* Cry, Cyt and parasporin toxins. *Toxins*, 6(9): 2732-2770.

Yamashita D, Sugawara T, Takeshita M, Kaneko J, Kamio Y, Tanaka I, Tanaka Y, Yao M (2014) Molecular basis of transmembrane beta-barrel formation of staphylococcal pore-forming toxins. *Nature Communications*, Sep 29; 5: 4897.

Appendix A

The following figures include the photographs taken for the pore repair and endocytosis assays.

Pore- Repair Assay Photographs

Pore forming toxin: 100% Cry5B 1 Hr

	0hr		**24hr**	
	Normal	Leaking	Normal	Leaking
L4440	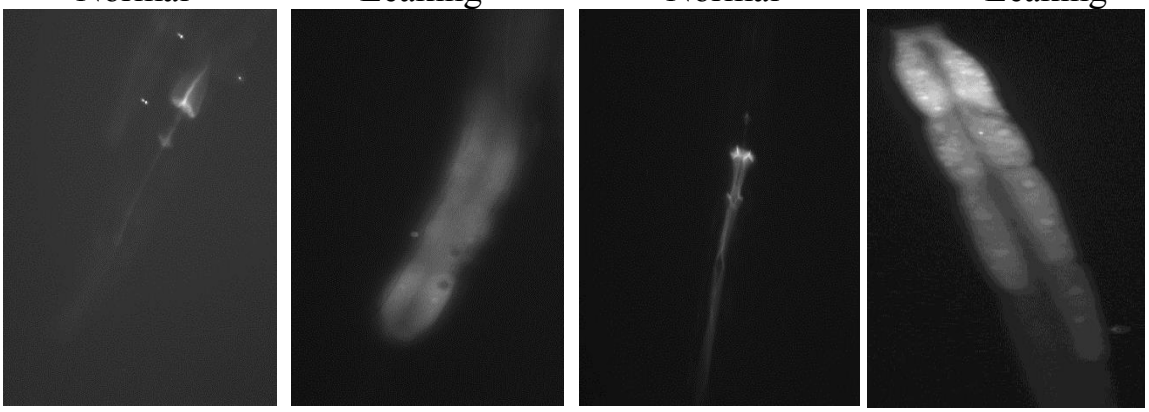			
Sek-1	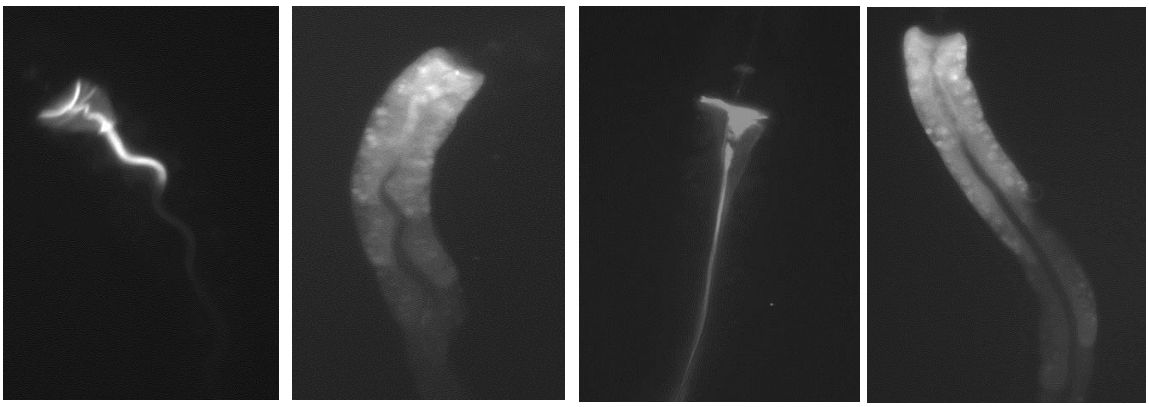			
Rab 11.1	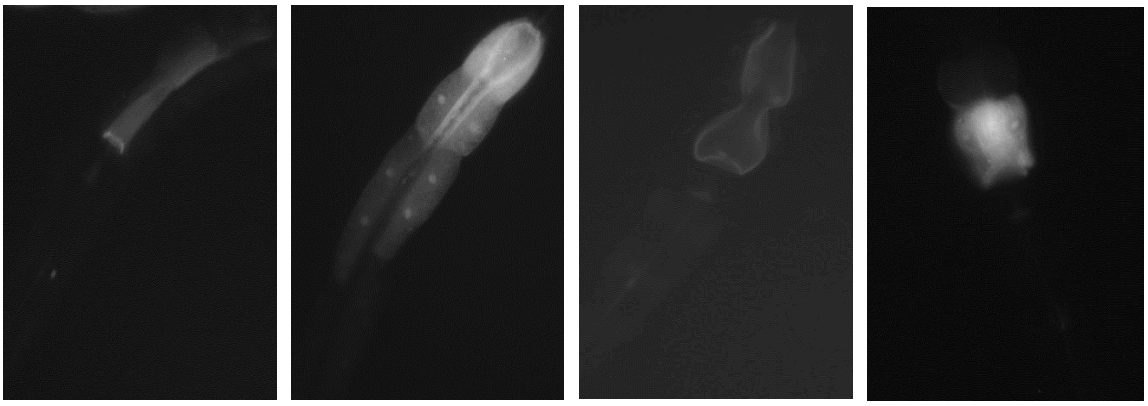			

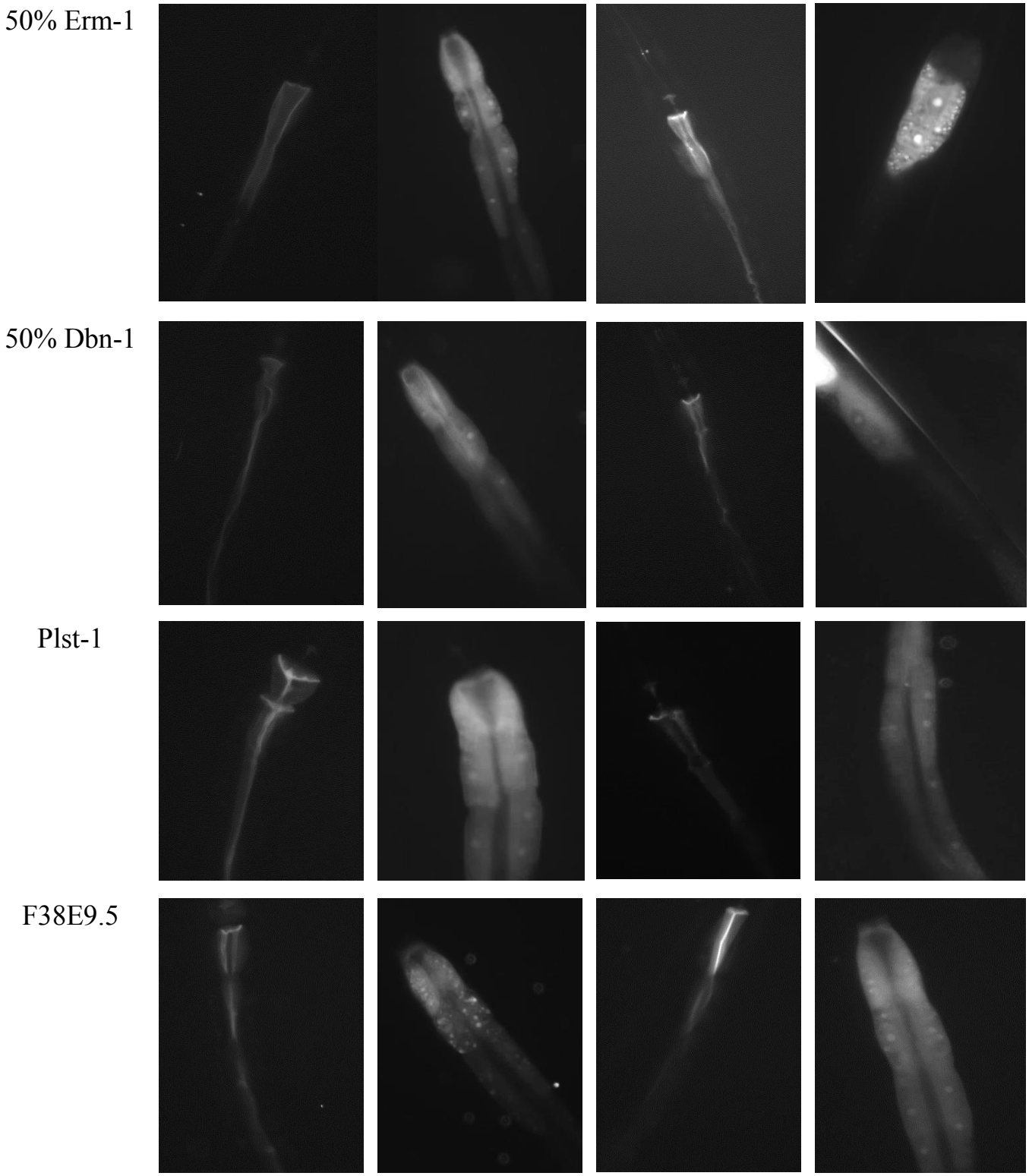

Appendix Figure-1: Pore Repair Assay. This figure compares photographs of worm intestines that show either an intact intestinal lumen (normal) vs. worms with pores that show leakage to the cytosol surrounding the intestinal epithelial cells (leaking). N=3

Endocytosis Assay Photographs

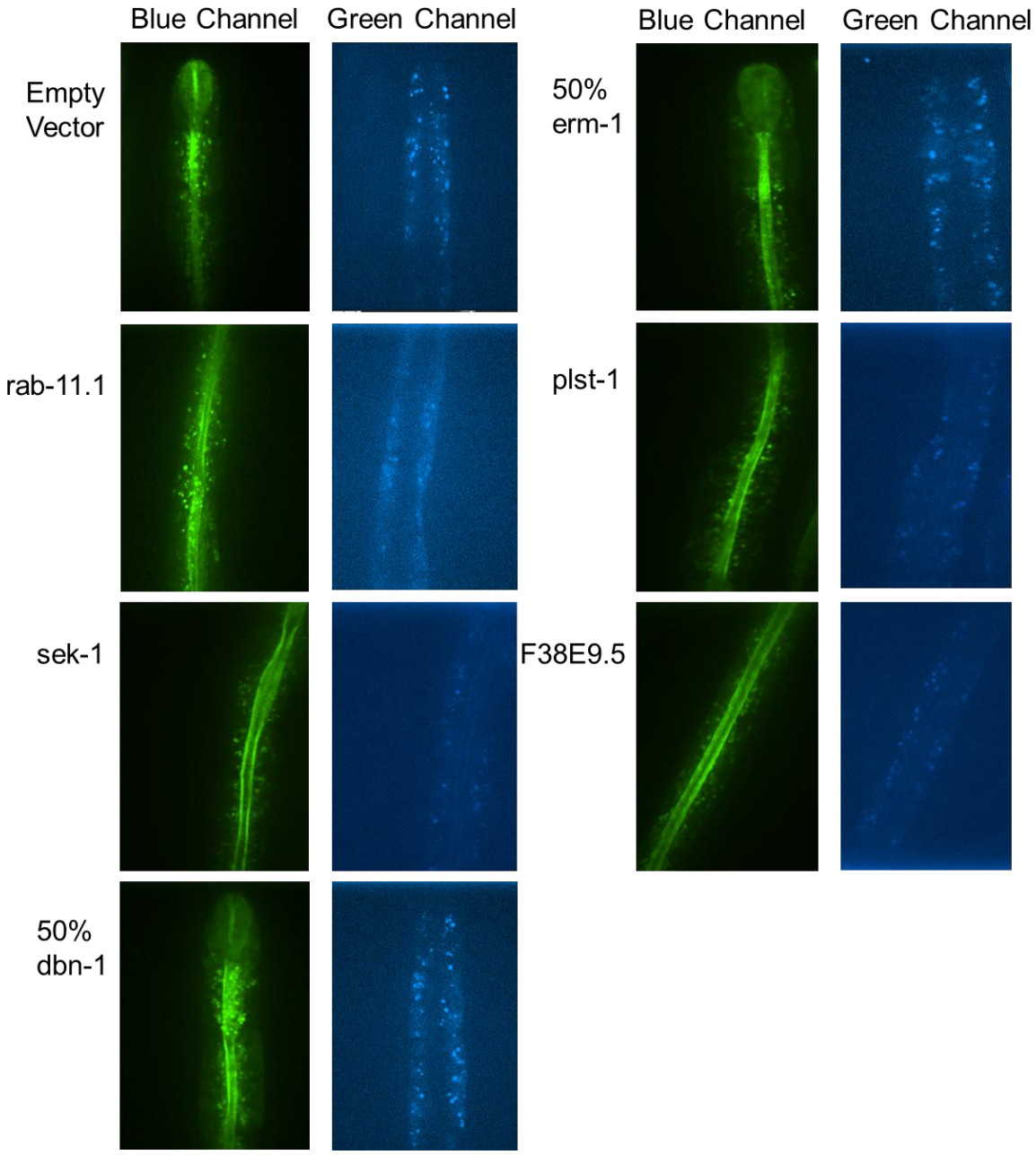

Appendix Figure-2: Pore Repair Assay. This figure compares photographs of worm intestines that show either vesicle formation and worm gut granules florescence (Green channel) or naturally fluorescing worm gut granules florescence (Blue channel). The florescent spots in each the green channel and the naturally fluorescing gut granules in the blue channel were counted to determine the percent of vesicle formation for each RNAi condition. N=3.